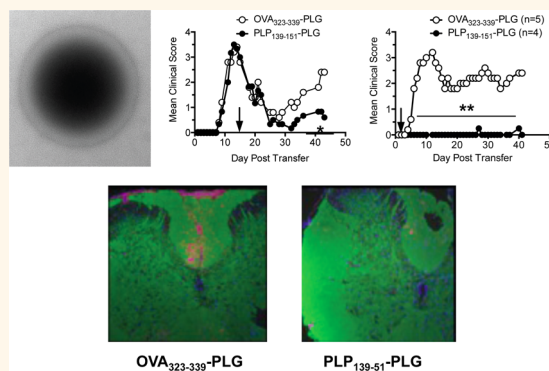


# A Biodegradable Nanoparticle Platform for the Induction of Antigen-Specific Immune Tolerance for Treatment of Autoimmune Disease

Zoe Hunter,<sup>†,§</sup> Derrick P. McCarthy,<sup>†,§</sup> Woon Teck Yap,<sup>‡,§</sup> Christopher T. Harp,<sup>†</sup> Daniel R. Getts,<sup>†</sup> Lonnie D. Shea,<sup>‡,\*</sup> and Stephen D. Miller<sup>†,\*</sup>

<sup>†</sup>Department of Microbiology-Immunology, Feinberg School of Medicine, Northwestern University, 6-713 Tarry Building, 303 East Chicago Avenue, Chicago, Illinois 60611, United States and <sup>‡</sup>Department of Chemical and Biological Engineering, Northwestern University, 2145 Sheridan Road, Evanston, Illinois 60208, United States. <sup>§</sup>Co-first authors contributed equally to this work.

**ABSTRACT** Targeted immune tolerance is a coveted therapy for the treatment of a variety of autoimmune diseases, as current treatment options often involve nonspecific immunosuppression. Intravenous (iv) infusion of apoptotic syngeneic splenocytes linked with peptide or protein autoantigens using ethylene carbodiimide (EDCI) has been demonstrated to be an effective method for inducing peripheral, antigen-specific tolerance for treatment of autoimmune disease. Here, we show the ability of biodegradable poly(lactic-co-glycolic acid) (PLG) nanoparticles to function as a safe, cost-effective, and highly efficient alternative to cellular carriers for the induction of antigen-specific T cell tolerance. We describe the formulation of tolerogenic PLG particles and demonstrate that administration of myelin antigen-coupled particles both prevented and treated relapsing-remitting experimental autoimmune encephalomyelitis (R-EAE), a CD4 T cell-mediated mouse model of multiple sclerosis (MS). PLG particles made on-site with surfactant modifications surpass the efficacy of commercially available particles in their ability to couple peptide and to prevent disease induction. Most importantly, myelin antigen-coupled PLG nanoparticles are able to significantly ameliorate ongoing disease and subsequent relapses when administered at onset or at peak of acute disease, and minimize epitope spreading when administered during disease remission. Therapeutic treatment results in significantly reduced CNS infiltration of encephalitogenic Th1 (IFN- $\gamma$ ) and Th17 (IL-17a) cells as well as inflammatory monocytes/macrophages. Together, these data describe a platform for antigen display that is safe, low-cost, and highly effective at inducing antigen-specific T cell tolerance. The development of such a platform carries broad implications for the treatment of a variety of immune-mediated diseases.



**KEYWORDS:** tolerance · anergy · regulatory T cells · autoimmune disease · PLG nanoparticles · experimental autoimmune encephalomyelitis · multiple sclerosis

Autoimmune diseases such as MS, rheumatoid arthritis, and type I diabetes (T1D) affect up to 23.5 million Americans and are one of the top 10 leading causes of death in females of all age groups up to 64. The estimated annual cost of treating autoimmune diseases is \$100 billion dollars, yet the standard therapies are not very effective and frequently invoke numerous undesirable side effects.<sup>1</sup> The current standard of therapy for autoimmune diseases seeks to broadly suppress the immune system, necessitating either the physical deletion

or inactivation of entire subsets of T cells. Attempts have been made to regulate autoimmune disease by inhibiting pathways involved in T cell activation and function such as the T cell receptor-CD3 signaling complex,<sup>2–6</sup> antigen presentation,<sup>7,8</sup> pro-inflammatory cytokine or chemokine production,<sup>9,10</sup> and T cell trafficking.<sup>11,12</sup> The nonspecific nature of these treatments may result in enhanced patient susceptibility to opportunistic infections, as illustrated by the rare, but often fatal, complications arising from the development of progressive multifocal

\* Address correspondence to s-d-miller@northwestern.edu.

Received for review September 26, 2013 and accepted February 23, 2014.

Published online February 24, 2014  
10.1021/nn405033r

© 2014 American Chemical Society

leukoencephalopathy following Tysabri (anti-VLA-4) or Rituximab (anti-CD20) therapy in a variety of clinical trials.<sup>13–16</sup>

Clearly, new strategies focused on the induction of long-term antigen-specific tolerance, rather than broad-based immunosuppression, need to be pursued for the treatment of human immune-mediated diseases. Numerous approaches using tolerance-based therapies to regulate human autoimmune diseases, including MS and T1D, have not yielded positive clinical outcomes.<sup>17,18</sup> As one example, a clinical trial in MS patients attempting to use an altered peptide ligand (APL) of a myelin basic protein (MBP) epitope to induce tolerance actually resulted in enhanced disease,<sup>19</sup> despite preclinical data showing that APLs were useful in treating the experimental EAE animal model of MS.<sup>20,21</sup> We have extensively investigated the use of apoptotic cells for the re-establishment of peripheral immune tolerance for therapy in rodent models of immune dysregulation and autoimmunity.<sup>17</sup> When administered *in vivo*, treatment with apoptotic cells is thought to recapitulate many of the basic mechanisms that maintain immune tolerance and homeostasis, such as the activation of Tregs, the production of immunosuppressive cytokines, and the induction of T cell anergy. These naturally occurring mechanisms can be exploited by chemically fixing autoantigen-pulsed splenocytes (Ag-SP) with ECDI, which facilitates rapid apoptosis and subsequent uptake and representation of autoantigen-decorated apoptotic debris by tolerogenic antigen presenting cells (APCs), thereby effectively inducing antigen-specific T cell tolerance in hosts with ongoing autoimmunity.<sup>22–24</sup> This strategy has been shown to be sufficient for both the prevention and treatment of relapsing EAE (R-EAE), a murine Th1/17-mediated model of MS,<sup>25</sup> and was the basis for a recently completed Phase I clinical trial in MS patients.<sup>26</sup> However, despite these successes, the reality of using cellular carriers for tolerance induction in the clinical arena is associated with the considerable cost and complexity of *ex vivo* laboratory manipulation and the high number of donor cells required. We recently showed that Ag-coupled to carboxylated 500 nm polystyrene nanoparticles served as a surrogate for apoptotic cellular carriers and induced tolerance for the prevention and treatment of R-EAE.<sup>27</sup> While these particles addressed the aforementioned concerns regarding cost and autologous donor cell requirements, they were not biocompatible or biodegradable and therefore did not provide a translatable, off-the-shelf alternative to ECDI-fixed donor cells.

The established success of PLG in the clinical setting led us to further investigate its potential as an antigen carrier for tolerance induction. Advancing the previous success we have reported using commercially available PLG particles for tolerance induction,<sup>27</sup> here we report the development of biodegradable PLG nanoparticles as antigen carriers capable of inducing robust

tolerance in the R-EAE mouse model. PLG particles were fabricated on-site by an emulsion process with modifications using poly(ethylene-co-maleic acid) as a surfactant (PLG-PEMA). The physical properties of the particles and their ability to couple peptides were characterized. Importantly, particles were investigated for their safety and ability to provide long-term protection from and treatment of R-EAE as characterized by clinical score, histology, and flow cytometric assessment of central nervous system (CNS) inflammatory cell infiltration. Treatment with myelin antigen coupled to PLG-based particles resulted in complete long-term protection from disease, as opposed to the partial protection provided by antigen coupled to polystyrene and commercially available PLG particles. This protection was characterized by minimal inflammatory cell infiltration, inflammatory cytokine production, and demyelination in the CNS of treated animals. Together, these studies highlight the therapeutic potential of a cost-effective, GMP-quality, biodegradable nanoparticle platform capable of peptide display for the induction of antigen-specific T cell tolerance.

## RESULTS AND DISCUSSION

**PLG Nanoparticle Synthesis and Characterization.** By exploiting naturally occurring debris clearance mechanisms, apoptotic antigen-coupled splenocytes are taken up by APCs without immune activation and the antigens are cross-presented to T cells to induce antigen-specific immune tolerance.<sup>28,29</sup> We have also recently shown that a carboxylated polystyrene nanoparticle platform can be used as a surrogate for apoptotic cells to carry antigen for efficient tolerance induction.<sup>27</sup> It was crucial, however, to move toward a more clinically translatable therapy. PLG particles have been used previously as adjuvants for immunization and as carriers of encapsulated antigen, highlighting their biodegradability.<sup>30,31</sup> We had also recently shown that commercially available carboxylated PLG nanoparticles coupled with peptides could induce immune tolerance,<sup>27</sup> but the tolerogenic efficiency was highly variable based on batch (data not shown). We thus manufactured PLG nanoparticles similar in size and surface charge to the polystyrene prototype, and tested whether the resultant particles could be used to display coupled peptide antigens for use as a reliable therapeutic tolerogenic agent.

Biodegradable PLG-PEMA nanoparticles were characterized by transmission electron microscopy and dynamic light scattering, both of which indicated a mean diameter between 400 and 500 nm (Figure 1A,B). Population analyses by dynamic light scattering established that the z-average diameter of the PLG-PEMA particles was 429.9 nm, slightly smaller than the z-average diameter of commercially available PLG particles (624.3 nm) available from Phosphorex (Figure 1C). Polystyrene beads (PS) with a z-average diameter of 503.6 nm were also used as controls. Covalent linkage

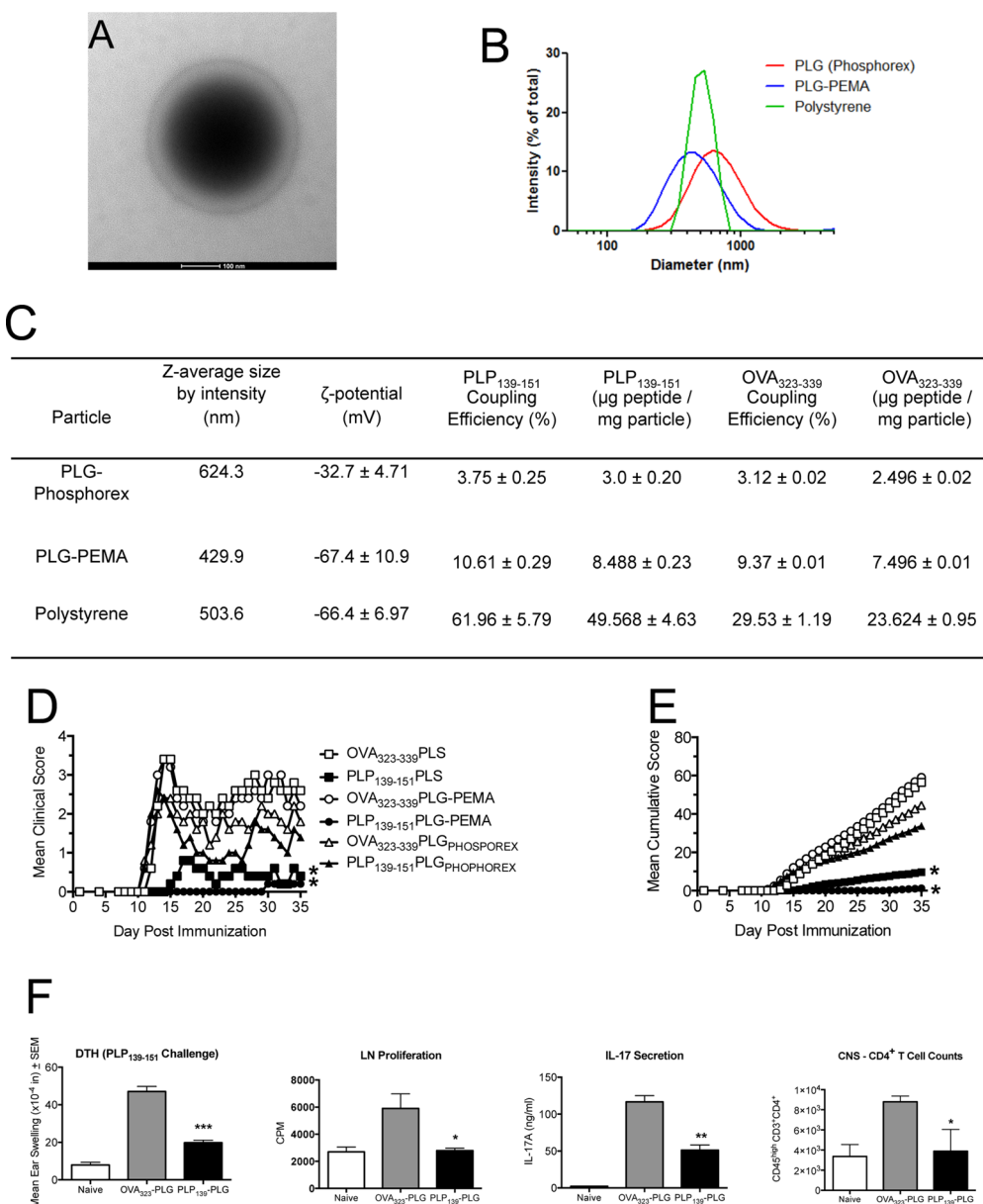


**Figure 1.** Peptide-coupled PLG-PEMA nanoparticles are efficient carriers for induction of antigen-specific tolerance for prevention of EAE. (A) Micrograph of PLG-PEMA particles. (B and C) Size distribution, average size (nm),  $\zeta$ -potential (mV), peptide coupling efficiency (%), and amount of OVA<sub>323-339</sub> and PLP<sub>139-151</sub> peptides coupled per milligram of PLG-PEMA particles prepared in the laboratory in comparison to PLG particles purchased from Phosphorex (PLG<sub>PHOSPHOREX</sub>) and polystyrene (PS) particles purchased from Polysciences. (D and E) Groups of 6–8 week old SJL/J mice were injected intravenously (iv) with 1.25 mg of the various carboxylated nanoparticles coupled to OVA<sub>323-339</sub> or PLP<sub>139-151</sub> 7d prior to induction of EAE by subcutaneous (sc) immunization with PLP<sub>139-151</sub>/CFA. Disease symptoms were scored by daily assessment of mean clinical score (D) as well as the mean cumulative clinical score (E) for the next 35 days. All experimental groups consisted of 5–7 mice and are representative of three separate experiments. Mean clinical scores and mean cumulative clinical scores for the mice tolerized with PLP<sub>139-151</sub> coupled to either PLG-PEMA or PS were significantly less than scores for mice treated with the appropriate OVA<sub>323-339</sub> coupled control particles (\*p ≤ 0.05, ANOVA). (F) At day +14, 24 h DTH responses to ear challenge with 10  $\mu\text{g}$  of PLP<sub>139-151</sub> were determined in 4–5 selected mice from the PLG-PEMA treated groups, and proliferative and IL-17 responses of draining lymph node T cells were determined following 72 h *in vitro* stimulation with peptide. At the end of the clinical observation period, the numbers of CNS-infiltrating T cells were enumerated in 3–4 selected mice from each group. Responses in PLP<sub>139-151</sub>-PLG treated mice were significantly less than those in OVA<sub>323-339</sub>-PLG treated controls (\*\*p ≤ 0.05, \*\*\*p ≤ 0.01, \*\*\*p ≤ 0.001, ANOVA).

of proteins/peptides to the surface of the PLG and PS particles using ECDI is critically dependent upon the surface density of carboxylate groups. Therefore, we investigated the surface density of carboxylate groups on the various particles using  $\zeta$ -potential as a relative

measure of the surface density of carboxylate groups. The  $\zeta$ -potential of the PLG-PEMA nanoparticles was found to be -67.4 ± 10.9 mV, significantly lower than the  $\zeta$ -potential of the commercial PLG particles measured at -32.7 ± 4.71 mV (Figure 1C).

**Myelin Peptide-Coupled PLG-PEMA Nanoparticles Prevent EAE in an Antigen-Specific Manner.** Due to the PLG-PEMA nanoparticles being similar in size to commercially available PLG and PS prototypes, and more heavily carboxylated than the commercially available PLG, we anticipated that we could achieve successful coupling of peptide antigens to the particle surface and that the antigen-coupled PLG particles could induce immune tolerance in the R-EAE disease model of MS. R-EAE is induced in SJL/J mice by subcutaneous immunization with the immunodominant proteolipid protein peptide sequence 139–151 (PLP<sub>139–151</sub>) emulsified in Complete Freund's Adjuvant (CFA). PLP<sub>139–151</sub> reactive T cells primed in the lymph nodes draining the site of immunization differentiate into Th1/Th17 effector cells and traffic to the CNS where they are reactivated by CNS-resident APCs to induce local inflammation and the recruitment of macrophages, monocytes, and neutrophils that nonspecifically mediate destruction of the myelin sheaths. The damage that ensues propagates the autoimmune response through the release, acquisition, and presentation of previously unrecognized antigens to T cells *via* a process known as epitope spreading.<sup>32</sup> We sought to compare the efficacy of 1.25 mg of PS, commercial PLG (PLG<sub>PHOSPHOREX</sub>) and PLG-PEMA particles ECDI-coupled with either PLP<sub>139–151</sub> or OVA<sub>323–339</sub> administered iv to SJL/J mice on day −7 relative to active R-EAE induction with PLP<sub>139–151</sub>/CFA. PLP<sub>139–151</sub>-coupled PLG-PEMA particles proved to be

significantly more effective in preventing onset of R-EAE as measured by both mean clinical score (Figure 1D) and mean cumulative disease scores (Figure 1E). Interestingly, the PLP<sub>139–151</sub>-PLG-PEMA particles outperformed the PLP<sub>139–151</sub>-PS treatment, despite having a slightly higher  $\zeta$ -potential and significantly lower PLP<sub>139–151</sub> coupling efficiency (Figure 1C). The PLG<sub>PHOSPHOREX</sub> particles were consistently less effective than PLG-PEMA particles in attenuating clinical symptoms of R-EAE, likely related to their higher  $\zeta$ -potential and decreased ability to be coupled with peptide. Prophylactic tolerance (day −7 relative to immunization) induced with PLP<sub>139–151</sub>-PLG-PEMA particles significantly inhibited development of PLP<sub>139–151</sub>-specific delayed-type hypersensitivity (DTH), an *in vivo* measure of Th1 activity, as well as proliferative responses and IL-17 production of draining lymph node T cells, and infiltration of T cells into the CNS (Figure 1F).

From this point forward, we chose to exclusively use PLG-PEMA particles (hereafter referred to more briefly as PLG), as they represent a biodegradable, PLG-based particle capable of preventing clinical symptoms of R-EAE as well as or better than the polystyrene prototype. We next investigated the optimal route of administration to prevent development of R-EAE. Using the standard dose of 1.25 mg of PLP<sub>139–151</sub>-coupled particles, we show that iv administration (Figure 2A) is significantly more effective at preventing clinical R-EAE symptoms than the intraperitoneal (ip) route

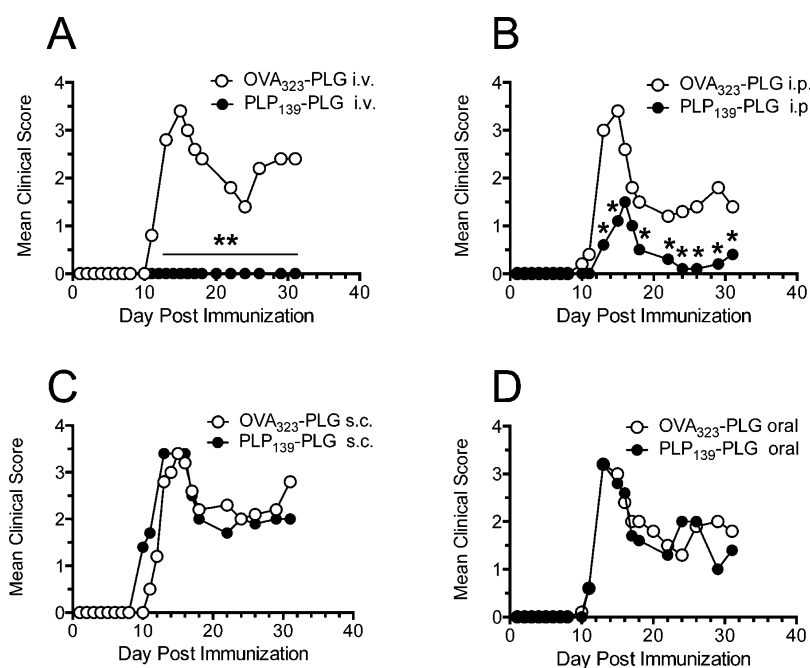


**Figure 2. Efficient induction of tolerance with peptide-coupled PLG-PEMA nanoparticles is dependent on route of administration.** The 6–8 week old female SJL/J mice were treated with 1.25 mg of PLG-PEMA nanoparticles coupled with OVA<sub>323–339</sub> or PLP<sub>139–151</sub> *via* intravenous (iv) (A), intraperitoneal (ip) (B), subcutaneous (sc) (C), or oral (D) routes of administration 7d prior to induction of EAE by sc immunization with PLP<sub>139–151</sub>/CFA. Disease symptoms were scored by daily assessment of mean clinical scores for the next 32 days. Data represent one of two representative experiments. Mean clinical scores were significantly less for mice treated with PLP<sub>139–151</sub>-PLG than for mice treated with the OVA<sub>323–339</sub>-coupled control PLG particles (\* $p \leq 0.05$ , \*\* $p \leq 0.01$  ANOVA).

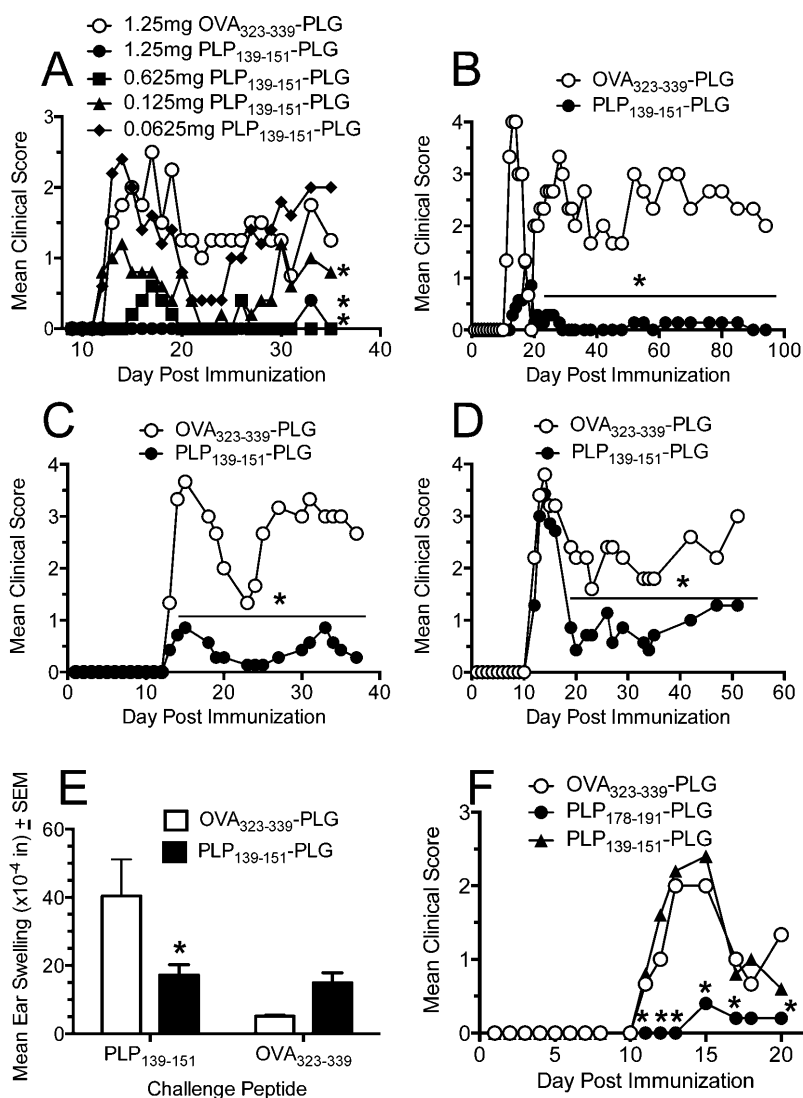


**Figure 3. Preventative treatment with myelin antigen-coupled PLG-PEMA nanoparticles induces long-term, antigen-specific tolerance.** (A) Optimal dosing of Ag-PLG-PEMA for preventative tolerance was determined by iv administration of increasing amounts of PLP<sub>139-151</sub>-PLG to SJL/J mice 7 days prior to disease induction by sc immunization with PLP<sub>139-151</sub>/CFA. Mice were monitored for development of clinical disease for 35 days after priming. (B–D) Duration of tolerance in mice was determined by iv administration of 1.25 mg of PLP<sub>139-151</sub>- or OVA<sub>323-339</sub>-PLG nanoparticles to 6–8 week old naïve female SJL/J mice which were primed sc with PLP<sub>139-151</sub>/CFA 7 days (B), 25 days (C), or 50 days (D) later. Mice were scored for development of clinical disease for the indicated time periods. (E) On day 8 relative to PLP<sub>139-151</sub>/CFA priming, DTH responses, as measured by 24 h swelling responses induced by sc ear challenge with PLP<sub>139-151</sub> or OVA<sub>323-339</sub> control peptide, in representative animals from panel B were determined. (F) The 6–8 week old SJL/J mice were treated iv with 1.25 mg of OVA<sub>323-339</sub>-PLG, PLP<sub>178-191</sub>-PLG, or PLP<sub>139-151</sub>-PLG 7 d prior to sensitization with PLP<sub>178-191</sub>/CFA, and disease was monitored for 35 days thereafter. All experimental groups consisted of 5–7 mice and are representative of 2–3 repeats. Differences in mean clinical scores and DTH responses were significantly less than the responses in groups tolerized with the irrelevant OVA<sub>323-339</sub>-PLG nanoparticles (\* $p \leq 0.05$ , ANOVA).

(Figure 2B), and that no protection was provided by Ag-coupled particles administered *via* the subcutaneous or oral routes (Figure 2C,D). In fact, sc administration of PLP<sub>139-151</sub>-PLG particles routinely led to a disease onset 1–2 days earlier than in animals treated with control OVA<sub>323-339</sub>-PLG. This result is consistent with previous observations showing a requirement for targeting of carboxylated coupled PS nanoparticles to MARCO<sup>+</sup> tolerogenic APCs in the spleen and liver.<sup>24,27</sup>

Following a dose titration experiment to confirm that our previously established dose of 1.25 mg of

PLP<sub>139-151</sub>-PLG particles was indeed optimal for disease prevention (Figure 3A), we next asked how long preventative tolerance could be maintained *in vivo* prior to disease induction. Six to eight week old female SJL/J mice were treated with either PLP<sub>139-151</sub>- or OVA<sub>323-339</sub>-PLG on day -7, day -25, or day -50 relative to active EAE induction. Treatment with PLP<sub>139-151</sub>-PLG on day -7 (Figure 3B) and day -25 (Figure 3C) prior to EAE induction resulted in near complete protection from disease. Interestingly, mice tolerized 50 days prior to disease induction showed no

protection from the acute phase of disease, but experienced reduced severity of disease during remission and relapse (Figure 3D). To determine the duration of protection afforded by PLP<sub>139–151</sub>-PLG administered at day –7 relative to EAE induction, a cohort of mice were scored up to 100 days postpriming. Figure 3B shows that protection from R-EAE was maintained for the entire experimental course as opposed to OVA<sub>323–339</sub>-PLG tolerized controls, which presented with a typical relapsing disease course for the duration of the experiment.

To determine if antigen-specific T cell tolerance was induced by Ag-PLG administered on day –7 relative to induction of EAE with PLP<sub>139–151</sub>, DTH responses were examined on day +8. PLP<sub>139–151</sub>-PLG treated mice showed reduced DTH reactivity when challenged subcutaneously with soluble PLP<sub>139–151</sub>, with net changes in ear swelling comparable to those following challenge with OVA<sub>323–339</sub> peptide (Figure 3E). As a proof of principle that tolerance induction using this method is not limited to a single peptide epitope and to test if bystander suppression was induced, we also demonstrated that prophylactic administration of PLP<sub>178–191</sub>-PLG, but not PLP<sub>139–151</sub>-PLG or OVA<sub>323–339</sub>-PLG, protects from active R-EAE symptoms induced with PLP<sub>178–191</sub>/CFA (Figure 3F). This indicates that tolerance is exquisitely peptide-specific in that tolerance to the dominant PLP<sub>139–151</sub> epitope did not induce cross-protection to disease induced by the PLP<sub>178–191</sub> epitope. Utilizing fluorescently labeled PLG-PEMA particles, we observed the particles mainly localized to the spleen, liver, and lung at 3, 6, and 18 h postinjection, but were largely undetectable in these organs by 24 h (manuscript in preparation).

**Myelin Peptide-Coupled PLG-PEMA Nanoparticles Can Safely Be Used To Treat Established R-EAE.** To determine the potential translational relevance of the Ag-PLG tolerance procedure for treating established autoimmune disease, we next sought to determine if therapeutic administration of Ag-PLG would be effective in treating mice with existing symptoms of EAE. For these experiments, we induced EAE via adoptive transfer of PLP<sub>139–151</sub> activated CD4<sup>+</sup> T cell blasts into naïve SJL mice as previously described.<sup>24,27</sup> Mice were tolerized shortly after adoptive disease transfer (day +2, Figure 4A) or at the peak of acute disease (day +14, Figure 4B). Similar to the prophylactic tolerance studies, mice treated with PLP<sub>139–151</sub>-PLG particles vs OVA<sub>323–339</sub>-PLG two days post adoptive transfer were totally protected from EAE as determined by clinical scores, and remained disease-free throughout the 40 day observation period, importantly indicating that tolerance could effectively down-regulate activated encephalitogenic T cells. At day 42 following adoptive transfer, brain and spinal cord tissue was collected and processed for histological analysis to determine the extent of cellular infiltration and demyelination in the CNS in tolerized animals.

CD45<sup>+</sup> inflammatory cell infiltration was particularly pronounced in the spinal cord of mice tolerized with control OVA<sub>323–339</sub>-PLG, while mice tolerized with PLP<sub>139–151</sub>-PLG had significantly less CD45 infiltration in the brain and spinal cord (Figure 4C). These trends were also true of CD3<sup>+</sup>CD4<sup>+</sup> T cell infiltration into the CNS (data not shown).

Mice treated therapeutically at peak disease (day +14) with PLP<sub>139–151</sub>-PLG particles (Figure 4B) reached complete remission (score 0) within one week of treatment, and did not experience any relapses as opposed to recipients of control OVA<sub>323–339</sub>-PLG particles. Spinal cord tissue was collected from these mice on day 44 and processed for histological analysis (Figure 4D, Figure S1). Luxol Fast Blue was used to visualize the extent of demyelination in treated animals. In accordance with reduced clinical disease symptomatology, mice tolerized with PLP<sub>139–151</sub>-PLG showed less demyelination (red arrows) and cellular infiltration (green arrows) than OVA<sub>323–339</sub>-PLG tolerized controls. This result is particularly interesting as all mice were of similar disease severity at time of tolerance induction, indicating that there continues to be considerable damage accrued during relapse and/or that PLP<sub>139–151</sub>-PLG tolerance therapy may stimulate myelin repair.

During the peak of acute PLP<sub>178–191</sub>-induced R-EAE, T cells reactive to PLP<sub>139–151</sub> are primed directly in the CNS as a result of intramolecular epitope spreading, leading to further inflammation and a primary relapse in clinical symptoms within days of disease remission.<sup>33</sup> To investigate whether tolerance could be induced therapeutically during disease remission to limit epitope spreading and thus prevent disease relapses, active R-EAE was induced by priming SJL/J mice with PLP<sub>178–191</sub>/CFA. Mice were then treated during disease remission (day +18) with PLG particles coupled to either OVA<sub>323–339</sub> or the spread epitope, PLP<sub>139–151</sub>. Mice tolerized with PLP<sub>139–151</sub>-PLG during disease remission experienced a significant reduction in severity of disease relapse indicating specific inhibition of epitope spreading (Figure 4E).

We have previously reported that mice with actively induced R-EAE treated by the iv administration of soluble antigen at or shortly after the peak of acute disease were susceptible to severe IgE-associated anaphylactic shock-associated mortalities.<sup>34</sup> To investigate whether this was also a possible consequence of late administration of myelin antigen-coupled PLG particles, we induced active PLP<sub>139–151</sub> R-EAE in female SJL/J mice on day 0, and tolerized the animals shortly after remission from acute disease (day 21) with either soluble PLP<sub>139–151</sub> or OVA<sub>323–339</sub>, or PLG-coupled PLP<sub>139–151</sub> or OVA<sub>323–339</sub>. Anaphylaxis is an acute, life-threatening phenomenon characterized by respiratory distress, erythema, decreased body temperature, unresponsiveness, and often death. As decreased body temperature is one

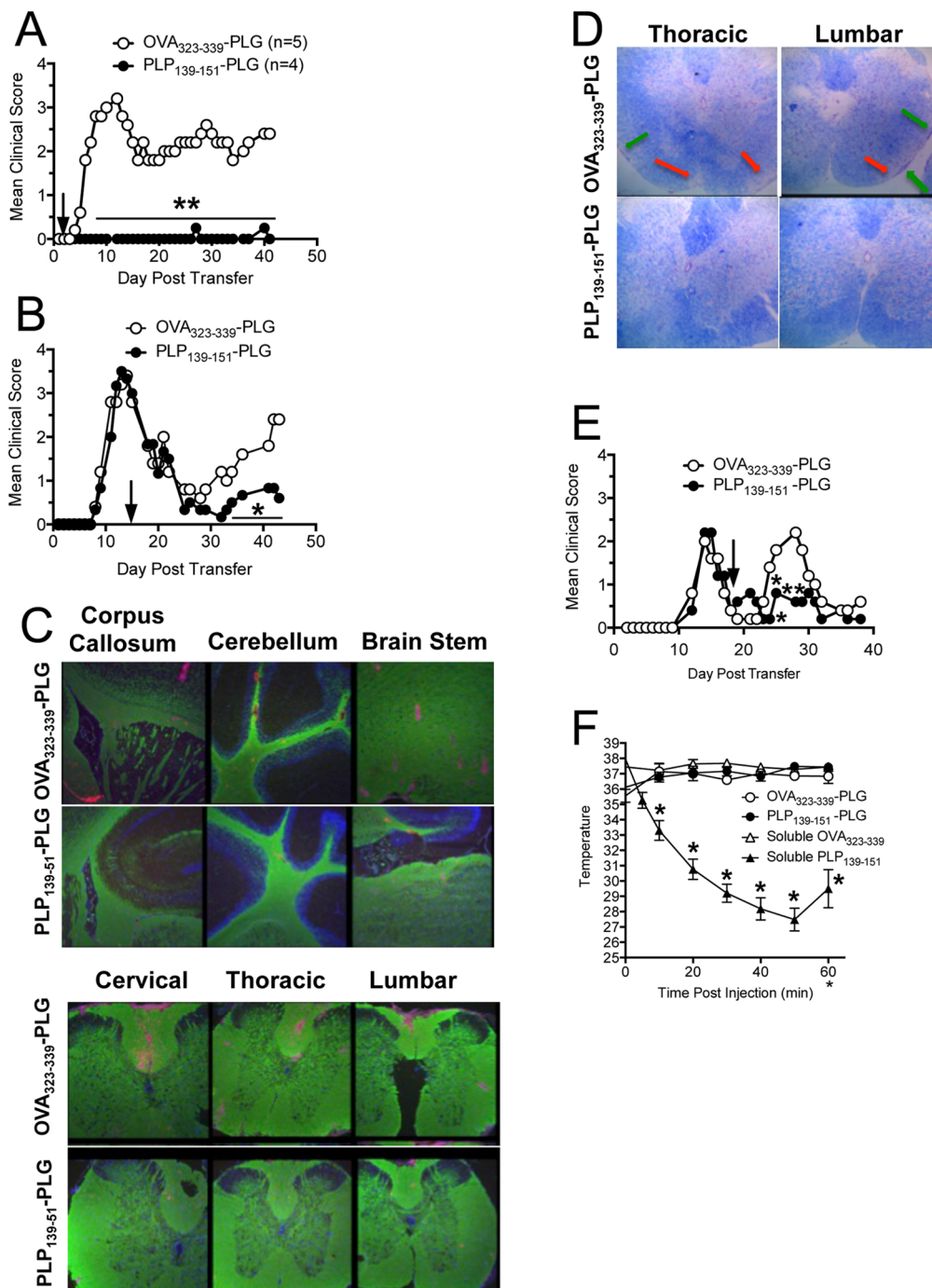


**Figure 4. Myelin Ag-coupled PLG-PEMA nanoparticles safely and effectively treat established EAE and prevent disease relapses.** EAE was induced in 6–8 week old female SJL/J mice by adoptive transfer of  $2.5 \times 10^6$  PLP<sub>139–151</sub>-specific blasts. Mice were injected iv with either 1.25 mg of OVA<sub>323–339</sub> or PLP<sub>139–151</sub>-PLG-PEMA nanoparticles 2 days (A) or 14 days (B) following cell transfer and mice were followed for clinical disease for the indicated number of days. (C) Brain and spinal cords were collected from the mice in panel A tolerized with OVA<sub>323–339</sub> or PLP<sub>139–151</sub>-PLG on day +2 for histological analysis on day 42, and sections were stained for PLP protein (green) and CD45 (red). (D) Spinal cord sections from mice from panel B were stained with Luxol Fast Blue. Areas of demyelination are indicated by red arrows; areas of cellular infiltration are indicated by green arrows. Higher magnification images are shown in Figure S1. (E) To test the efficacy of Ag-PLG nanoparticles to treat EAE mice during disease remission for prevention of disease relapses, SJL/J mice with EAE induced by sc priming with PLP<sub>178–191</sub>/CFA were tolerized by iv infusion of OVA<sub>323–339</sub> or PLP<sub>139–151</sub>-PLG on day +18, and clinical disease was scored for an additional 21 days. (F) To determine the potential of Ag-PLG tolerance to trigger anaphylaxis in primed mice, EAE was induced in 6–8 week old female SJL/J mice by subcutaneous injection of PLP<sub>139–151</sub>/CFA and the mice were treated by iv infusion of 200  $\mu$ g of soluble OVA<sub>323–339</sub> or PLP<sub>139–151</sub>, or the same peptides coupled to PLG-PEMA nanoparticles on day +21. Temperature of the injected animals was monitored and recorded every 10 min for 1 h following injection as a measure of induction of anaphylaxis. All experimental groups consisted of 5–7 mice and are representative of 2–3 separate experiments. Mean clinical scores were significantly less for mice treated with PLP<sub>139–151</sub>-PLG than for mice treated with the OVA<sub>323–339</sub>-coupled control PLG particles (\*p ≤ 0.05, \*\*p ≤ 0.01 ANOVA).

measurable trait of anaphylactic reaction, all mice were implanted with subcutaneous temperature transponders three days prior to tolerance induction so that body temperatures could be measured using a programmable temperature transponder pocket scanner (BioMedic Data Systems, Maywood, NJ). Temperatures were obtained at 5 and 10 min following injection, and then at 10 min intervals for a total of 60 min. Mice administered soluble PLP<sub>139–151</sub> experienced drastic decreases in core temperature immediately following injection (Figure 4F). Three out of five mice in the soluble PLP<sub>139–151</sub> group died before the 60 min time point. The core temperatures of the remaining two mice began to increase after 50 min, and subsequently restabilized. In stark contrast, mice given PLP<sub>139–151</sub>-PLG maintained stable body temperatures throughout the observation time course. We continued to score both the soluble PLP<sub>139–151</sub> and the PLP<sub>139–151</sub>-PLG groups after tolerance induction. Interestingly, while both groups experienced similar disease severity during the peak acute phase of disease, as well as complete remission, only mice tolerized with PLP<sub>139–151</sub>-coupled PLG particles were able to remain in remission, while mice treated with the soluble peptide relapsed within four days (data not shown). These results thus indicate the efficacy and safety of Ag-PLG tolerance for treatment of established R-EAE. A similar safety profile has been observed in OVA/alum primed mice with pre-existing OVA-specific IgE upon iv treatment with OVA-PLG (in preparation).

**Treatment with Peptide-Coupled PLG-PEMA Nanoparticles Reduces Immune Cell Infiltration and Cytokine Production in the CNS.** To further characterize the immune cell populations accessing the CNS following treatment with antigen-coupled PLG nanoparticles, we analyzed CNS cellular infiltrates by flow cytometric analysis (Figure 5A) of mice with adoptive transfer R-EAE tolerized with either OVA<sub>323–339</sub>- or PLP<sub>139–151</sub>-PLG on day +2 following transfer of PLP<sub>139–151</sub>-specific T cell blasts (Figure 4A). Lymphocytes, APC subsets, and microglia were all significantly reduced at peak disease in the CNS of PLP<sub>139–151</sub>-PLG treated mice (Figure 5B–D). Within the APC subsets, monocytes/macrophages (CD45<sup>hi</sup>CD11b<sup>hi</sup>CD11c<sup>lo</sup>), plasmacytoid dendritic cells (pDC) (CD45<sup>hi</sup>CD11b<sup>low</sup>CD11c<sup>hi</sup>), and CD11b<sup>+</sup> dendritic cells (CD45<sup>hi</sup>CD11b<sup>hi</sup>CD11c<sup>hi</sup>) were all reduced in PLP<sub>139–151</sub>-PLG tolerized mice as compared to the OVA<sub>323–339</sub>-PLG tolerized controls (Figure 5E–G). Consistent with the profound protection from clinical symptoms of disease (Figure 4A), intracellular cytokine staining revealed a significant reduction in the numbers of both encephalitogenic Th1 (IFN- $\gamma$ <sup>+</sup>) and Th17 (IL-17A<sup>+</sup>) CNS-infiltrating T cells in PLP<sub>139–151</sub>-PLG tolerized mice compared to OVA<sub>323–339</sub>-PLG tolerized controls (Figure 5H, Figure S2).

We have recently demonstrated the effective use of carboxylated 500 nm polystyrene nanoparticles linked to autoantigenic peptide epitopes as a platform for the

induction of immunological tolerance for the prevention and treatment of the EAE model of MS.<sup>27</sup> This material served as an excellent substitute for Ag-coupled apoptotic splenocytes (Ag-SP), since (1) the negative charge on these nanoparticles was ideal for allowing the covalent attachment of peptides via ECDI chemistry; (2) the size of the particles mimicked apoptotic fragments; and (3) antigen-coupled polystyrene nanospheres were successful surrogates for Ag-SP as they stimulated uptake by APCs in the splenic marginal zone through the scavenger receptor MARCO, promoted Treg activation, and inhibited the differentiation of Th1/Th17 effector cells through the induction of T cell anergy. Although tolerance induction with antigen-coupled polystyrene nanospheres efficiently inhibited the induction of EAE when administered prophylactically and abrogated ongoing disease when administered therapeutically, the translational potential of this platform is questionable due to the nonbiodegradable nature of the material and its potential toxicity.<sup>35</sup> Although numerous biodegradable polymers and copolymers abound, the copolymer PLG has been extensively studied in models of drug delivery and vaccine therapy due to its natural biologic compatibility. We therefore investigated the use of carboxylated PLG nanoparticles as a viable alternative to the polystyrene platform since PLG is biodegradable, FDA-approved, and could be manufactured with physical properties comparable to polystyrene nanoparticles in terms of diameter and surface charge. Similar to polystyrene particles, commercially available PLG nanoparticles conjugated to encephalitogenic epitopes ameliorated disease both prophylactically and therapeutically when administered to EAE mice,<sup>27</sup> and similar to tolerance induced by antigen-coupled polystyrene nanoparticles, their regulatory effects appear to require uptake via the MARCO scavenger receptor.<sup>36</sup> However, inconsistencies in the level of protection afforded by the administration of antigen coupled to commercially available PLG nanoparticles indicated a need for particle modifications.

In the present study, we report that PLG nanoparticles modified with the surfactant PEMA and covalently decorated with peptide antigen are a superior and more reliable platform for the induction of immunological tolerance when compared to polystyrene and commercially available PLG nanoparticles. Tolerance induction using this platform was most effectively induced via iv administration and was antigen-specific and safe (mice exhibited no symptoms of anaphylaxis when therapy was administered after peak of acute disease). In addition, tolerance induction by antigen-conjugated PLG-PEMA nanoparticles limited T cell recall responses in an antigen-specific manner, and drastically reduced the recruitment of innate and adaptive effector cells into the CNS following EAE induction. Furthermore, tolerance induced by antigen-conjugated PLG-PEMA

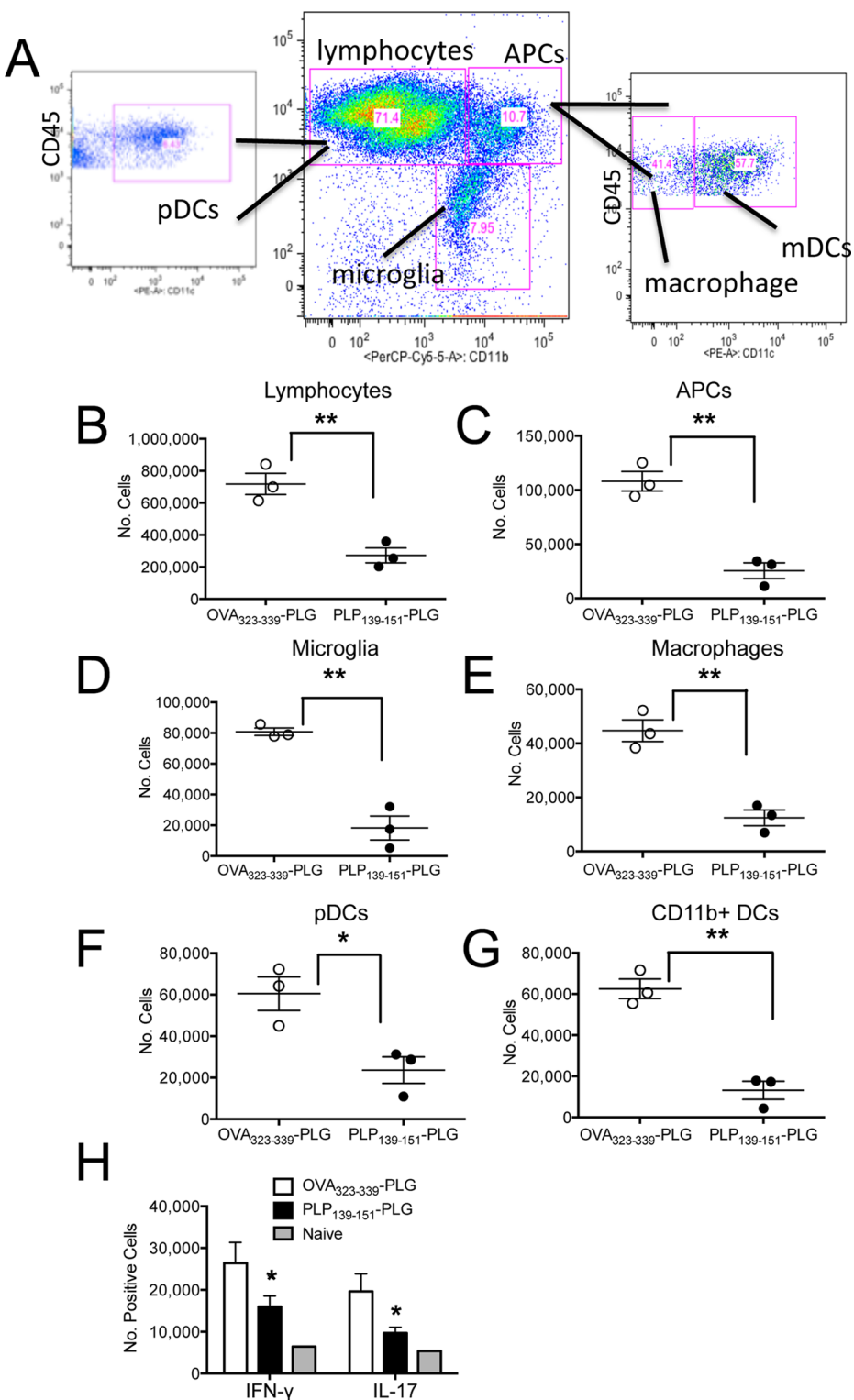


**Figure 5.** Induction of therapeutic tolerance with myelin Ag-coupled PLG-PEMA nanoparticles reduces CNS immune infiltration and cytokine secretion. (A) SJL/J mice were injected iv with PLG-PEMA nanoparticles coupled with OVA<sub>323–339</sub> or PLP<sub>139–151</sub> 2d following EAE induction by adoptive transfer of activated PLP<sub>139–151</sub>-specific T cell blasts. At the peak of disease in the OVA<sub>323–339</sub>-PLG treated controls (d+14), brains and spinal cords were removed and processed into single cell suspensions, and the numbers of infiltrating immune cells were analyzed by flow cytometry using the indicated gating scheme. The numbers of lymphocytes (B), APCs (C), microglia (D), macrophages (E), myeloid dendritic cells (mDCs) (F), and conventional peripheral dendritic cells (pDCs) (G) were enumerated by flow cytometry. (H) CNS cell preparations from the two treated groups as well as from naive controls were stimulated with PMA and ionomycin for 5 h prior to intracellular staining for IFN- $\gamma$  and IL-17A. Representative dot plots are shown in Figure S2. Data is representative of 2–3 separate experiments. Numbers of the various cell subsets infiltrating the CNS were significantly less for mice treated with PLP<sub>139–151</sub>-PLG than for mice treated with the OVA<sub>323–339</sub>-coupled control PLG particles (\* $p \leq 0.05$ , \*\* $p \leq 0.01$  ANOVA).

nano particles was long-lasting and durable, limiting the severity of EAE when administered over 50 days prior to disease induction, and maintaining protection from disease for up to 100 days post immunization. Finally, treatment with antigen-conjugated PLG-PEMA particles was also potent at inducing tolerance in disease mediated by the transfer of a large number of highly activated encephalitogenic T cells, demonstrating its potent therapeutic efficacy.

The mechanisms by which modification of PLG nanospheres with PEMA surfactant enhances their tolerogenic potential is worthy of discussion. Multiple factors are involved in influencing the uptake and immune recognition mediated by nanoparticles. These include particle size, shape, charge, polymer composition and route of administration, each of which dictate how the immune system responds to their recognition and the quality of the eventual response that is formed. In one set of studies, administration of PLG particles with diameters less than 500 nm was found to skew a Th2-type response normally induced by hepatitis B virus antigen toward a Th1 response, thereby exerting adjuvant-like effects.<sup>30,37</sup> Additionally, antigen encapsulated in <500 nm PLG particles were found to elicit potent cytotoxic T lymphocyte responses when administered *via* ip injection, whereas the same antigen encapsulated in PLG particles with diameters greater than 2.0  $\mu\text{m}$  did not.<sup>38</sup> Such differences in outcome may be attributed to the ability of APCs to recognize and internalize smaller particles by phagocytosis, while larger particles may only initiate APC recognition and adherence. This observation is likely of significant consequence to the platforms used in our tolerance induction model, since uptake of the particles and cross-presentation of the covalently linked antigen onto MHC class II molecules of recipient APCs is necessary to promote T cell anergy *via* the two-signal hypothesis.<sup>28,39</sup> Moreover, we have previously demonstrated that 500 nm polystyrene particles maximally induced tolerance when compared to particles of larger and smaller diameter.<sup>27</sup> However, size alone is unlikely to account for the superior effects of antigen-conjugated PLG-PEMA when compared to other platforms examined in this study. Little difference exists between the size of our custom particles and those commercially available, and similar phenomena have been reported in a prior study.<sup>40</sup> Of obvious consequence to the efficacy of our custom PLG nanoparticles is the addition of carboxyl groups through surface modification with the surfactant PEMA, as evidenced by the 2-fold increase in magnitude of  $\zeta$ -potential. Since ECDI chemistry forms covalent bonds between carboxyl groups and primary amines, this directly affects the amount of antigen that can be conjugated to the surface of the particles, resulting in a 3-fold increase in antigen dose administered by PLG-PEMA nanoparticles when compared to the commercially

available alternative. Yet, despite the similar magnitude in  $\zeta$ -potential between PLG-PEMA and polystyrene nanoparticles, PLG-PEMA consistently demonstrated a superior capacity to prevent and treat EAE across multiple experiments (data not shown), even though a higher antigen dose was administered upon treatment with polystyrene nanospheres. Thus, antigen dose appears to not be the sole determinant of increased efficacy in our tolerance induction platform.

Another important determinant in the immune recognition and uptake of nanoparticles may be shape. In one study, it was reported that shape of the biomaterial mediated the initiation of phagocytosis by professional APCs, while size of the nanoparticle determined the ability of the APC to complete phagocytosis.<sup>41</sup> Although surface modification with PEMA is unlikely to change the overall shape of the PLG nanoparticle, its increased negative charge may influence the conformation of PLG-antigen-PLG conjugates and dictate the size of the aggregates.<sup>40</sup> Thus, it is of interest to determine whether monodispersed antigen-conjugated PLG-PEMA can function as efficiently during immune recognition for the induction of immunological tolerance, or if the repeated motifs present in the PLG-antigen-PLG are necessary to direct the particles into a tolerogenic pathway *via* MARCO scavenger receptors.<sup>42</sup> This possibility is currently under investigation. Finally, the enhanced charge may not only affect recognition by APCs,<sup>43,44</sup> but it may also influence the adsorption of serum proteins and opsonins that have been demonstrated to have a profound effect on nanoparticle clearance and uptake by macrophages.<sup>45,46</sup>

With the surge in popularity of nanomaterials for use in drug delivery and vaccine therapy, there has been a recent interest in the use of nanoparticles for immunosuppression and peripheral tolerance induction. Zhao *et al.* demonstrated T cell tolerance for the treatment of EAE could be induced by subcutaneously injecting SJL/J mice with PLG particles encapsulating a bifunctional peptide inhibitor of T cell activation (PLP<sub>139–151</sub> conjugated to a CD11a peptide)<sup>47,48</sup> However, administration of the tolerogen induced anaphylaxis at day 45 with only 10% of the treated animals surviving, limiting the efficacy of this therapy. Significantly, our current results show that peptide-coupled PLG particles do not initiate anaphylaxis in primed mice (Figure 4F). Huang *et al.* reported that DNA/polyethyleneimine nanoparticles could prevent antigen-specific T cell responses by upregulating IDO production from dendritic cells and T<sub>REGS</sub>. This led to decreased CD4 and CD8 T cell responses and significantly limited joint inflammation in an experimental model of rheumatoid arthritis.<sup>49</sup> Yet whether treatment with DNA/polyethyleneimine nanoparticles truly induces antigen-specific tolerance is questionable since the response to unrelated antigens was not measured following treatment. Lastly, a study utilizing 60 nm

particles encapsulating a gold core conjugated to an encephalitogenic peptide and 2-(1'H-indole-3'-carbonyl)-thiazole-4-carboxylic acid methyl ester, an aryl hydrocarbon receptor (AhR) ligand, was able to induce T<sub>REG</sub>-mediated protection from EAE.<sup>50</sup>

## CONCLUSION

In summary, we describe a simple, yet highly efficacious, method for inducing potent T cell tolerance for the prevention *and* treatment of EAE employing iv infusion of antigen-coupled PLG-PEMA nanoparticles. Preliminary evidence indicates that similar to what we have published regarding antigen-coupled PSB,<sup>27</sup> tolerance induced by antigen-coupled PLG particles is

due to the combined effects of T cell anergy and the activation of Tregs. The safety, low-cost, and functionality of this protocol broadens its applicability in the clinical setting. By simply switching out the antigenic epitopes conjugated to the PLG-PEMA particles, the platform can easily be modulated to treat a wide variety of autoimmune and allergic diseases. This tolerance platform may also be useful for promoting the use of recombinant protein and gene therapy approaches in diseases characterized by protein lack or insufficiency by eliminating the induction of neutralizing immune responses in individuals receiving proteins to which they have never developed self-tolerance during development of the immune system.

## MATERIALS AND METHODS

**Mice.** Female SJL/J mice were purchased from Harlan Laboratories (Indianapolis, IN). All mice were housed under specific pathogen-free conditions in the Northwestern University Center for Comparative Medicine and maintained according to protocols approved by the Northwestern University Institutional Animal Care and Use Committee.

**Phosphorex PLG Nanoparticle Preparation.** The 500 nm poly(D,L-lactic-co-glycolic acid) (PLG) nanoparticles with surface carboxylate groups were purchased from Phosphorex, Inc. (Fall River, MA) and were resuspended to a final concentration of 25 mg/mL in sterile phosphate-buffered saline (PBS), pH 7.4. The resulting nanoparticle suspension was then filtered through a 40  $\mu$ m cell strainer, aliquoted into 500  $\mu$ L fractions, and stored at  $-20^{\circ}\text{C}$  until further use.

**PLG-PEMA Nanoparticle Synthesis.** PLG-PEMA nanoparticles were prepared using a single emulsion-solvent evaporation method. PLG with carboxylate end groups, a 50:50 D,L-lactide/glycolide ratio and inherent viscosity of 0.18 dL/g in hexafluoro-2-propanol was purchased from Lactel Absorbable Polymers (Birmingham, AL); PEMA [poly(ethylene-alt-maleic anhydride)] was purchased from Polysciences, Inc., Warrington, PA. Two milliliters of 20% (w/v) PLG in dichloromethane (DCM) (Sigma, St. Louis, MO) was added dropwise to 4 mL of 1% (w/v) aqueous PEMA, and the mixture was sonicated for 30 s at 100% amplitude using a Cole-Parmer CPX130 Ultrasonic Processor equipped with a Cole-Parmer CV 18 ultrasonic probe adapter and a Cole-Parmer 3 mm probe with stepped tip. Immediately after sonication, the emulsion was poured into 200 mL of 0.5% (w/v) aqueous PEMA under stirring on a Bellstir Multistir 9 magnetic stirrer. The resultant nanoparticles were stirred for 12 h to allow for the DCM to completely evaporate and were then washed three times in 0.1 M sodium carbonate-sodium bicarbonate buffer, pH 9.6. The particles were then resuspended in a 20 mL solution of 3% (w/v) aqueous D-mannitol and 4% (w/v) aqueous sucrose, gradually frozen to  $-80^{\circ}\text{C}$ , and lyophilized to dryness.

**Nanoparticle Size and  $\zeta$ -Potential Characterization.** Ten microliters of 25 mg/mL nanoparticle suspension was uniformly diluted with 990  $\mu$ L of 18.2 MΩ·cm water, and size and  $\zeta$ -potential were measured using dynamic light scattering (DLS) on the Zetasizer Nano ZS from Malvern Instruments, Inc. (Westborough, MA). Particle size as determined by DLS was confirmed by transmission electron microscopy. Particles were dried overnight on 400 mesh holey carbon copper grids and imaged directly on a FEI Tecnai Spirit G2 120 kV transmission electron microscope from FEI (Hillsboro, OR). Efficiency of peptide coupling was determined using radiolabeled peptides before and after incubation with 16.67 mg/mL of ECDI for 1 h at room temperature ( $21^{\circ}\text{C}$ ).

**Microscopy.** For particle tracking experiments, female SJL/J mice aged 6–10 weeks were injected iv with 6.25 mg of

fluorescently labeled PLG-PEMA (2% w/w coumarin-6) in PBS vehicle. At indicated time points (2–3 mice per time point), mice were sacrificed, and organs were harvested and flash frozen in OCT compound. Organ slices were prepared on a cryostat and counter stained with DAPI.

**Peptides.** PLP<sub>139–151</sub> (HSLGKWLGHDPDKF) and OVA<sub>323–339</sub> (ISQAVHAAHAEINEAGR) were purchased from Genemed Synthesis. PLP<sub>178–191</sub> (NTWTTCSIAFPSK) was purchased from Peptides International.

**Induction and Clinical Evaluation of Peptide-Induced EAE.** Peptide-induced and adoptive transfer EAE was induced in SJL/J mice as previously described.<sup>24,27,51</sup> Individual animals were observed daily and clinical scores were assessed on a 0–5 scale as follows: 0 = no abnormality; 1 = limp tail or hind limb weakness; 2 = limp tail and hind limb weakness; 3 = hind limb paralysis; 4 = hind limb paralysis and forelimb weakness; and 5 = moribund. The data are reported as the mean daily clinical score. Paralyzed animals were afforded easier access to food and water.

**Tolerance Induction with Antigen-Coupled PLG and Polystyrene Nanoparticles.** Peptide antigens were attached to the surface of 500 nm carboxylated PLG particles using ECDI (1-ethyl-3-(3'-dimethylaminopropyl)carbodiimide; EMD Chemicals, Inc., Gibbstown, NJ), with 0.08 mg of peptide in the presence of 0.32 mg ECDI/mg of PLG nanoparticles. Animals received intravenous injections of approximately  $9 \times 10^9$  nanoparticles comprising 10–15  $\mu\text{g}$  of peptide, depending on the sequence used in the coupling reaction. Carboxylated 500 nm polystyrene beads (PSBs) were purchased from Polysciences (Warrington, PA). Peptide antigens were attached to particles using ECDI according to manufacturer's instructions, in the same process and concentration as with the PLG nanoparticles.

**Delayed-Type Hypersensitivity (DTH) and *In Vitro* Proliferation Assays.** DTH was performed via a 24 h ear swelling assay as previously reported.<sup>52</sup> Prechallenge ear thickness was determined using a Mitutoyo model 7326 engineer's micrometer (Schlesinger's Tools, Brooklyn, New York). Immediately thereafter, DTH responses were elicited by injecting 10  $\mu\text{g}$  of peptide in 10  $\mu\text{L}$  of PBS into the dorsal surface of the ear using a 100  $\mu\text{L}$  Hamilton syringe fitted with a 30 gauge needle. The increase in ear thickness over prechallenge measurements was determined 24 h after ear challenge. Results are expressed in units of  $10^{-4}$  in.  $\pm$  SEM. For cell activation and proliferation assays, draining inguinal lymph nodes (LN)s and/or spleens were harvested from naïve mice or primed mice at the indicated times following disease induction, counted, and cultured in 96-well microtiter plates at a density of  $5 \times 10^5$  cells/well in a total volume of 200  $\mu\text{L}$  of HL-1 medium (BioWhittaker) containing 100 U/mL penicillin, 100  $\mu\text{g}/\text{mL}$  streptomycin, and 2 mM L-glutamine). Cells were cultured at  $37^{\circ}\text{C}$  with medium alone or with 10  $\mu\text{g}/\text{mL}$  of peptide Ag for 72 h. During the last 24 h, cultures were pulsed with 1  $\mu\text{Ci}/\text{well}$  [<sup>3</sup>H]TdR, and uptake was detected using a

Topcount microplate scintillation counter and results are expressed as mean of triplicate cultures.

**Antibodies and Flow Cytometry.** Cells were isolated from the CNS and stained as previously described.<sup>53</sup> FcR blocking with CD16/32 was performed followed by staining with various combinations of the following antibodies: αCD3-APC/Cy7, αCD11c-PE, αCD45-FITC, αIFN-γ-PE/Cy7, αIL-17-APC, (eBioscience), αCD4-Pacific Blue, and αCD11b-PerCP/Cy5.5 (Becton-Dickinson). Cytometric data were collected on a FACS Canto flow cytometer (Becton-Dickinson). DiVa software was used for data acquisition and analysis (Becton-Dickinson).

**Conflict of Interest:** The authors declare no competing financial interest.

**Acknowledgment.** Supported in part by NIH Grants EB013198 (S.M. and L.S.), NS-026543 (S.M.), and grants from the Myelin Repair Foundation (S.M.) and the Dunard Fund (S.M.). Z.H. and D.M. were supported by postdoctoral fellowship grants from the Paralyzed Veterans of America and NIH 5T32 DK077662, respectively.

**Supporting Information Available:** Figures show how induction of therapeutic tolerance with myelin Ag-coupled PLG-PEMA nanoparticles reduces (Figure S1) the number of demyelinating lesions and CNS-infiltrating cells and (Figure S2) cytokine-secreting Th1 and Th17 T cells in the CNS. This material is available free of charge via the Internet at <http://pubs.acs.org>.

## REFERENCES AND NOTES

1. American Autoimmune Related Diseases Association. The Cost Burden of Autoimmune Disease: The Latest Front in the War on Healthcare Spending; AARD: Eastpointe, MI, 2011. <http://www.aarda.org/pdf/cbad.pdf>.
2. Chatenoud, L.; Thervet, E.; Primo, J.; Bach, J. F. Anti-CD3 Antibody Induces Long-Term Remission of Overt Autoimmunity in Nonobese Diabetic Mice. *Proc. Natl. Acad. Sci. U.S.A.* **1994**, *91*, 123–127.
3. Chatenoud, L.; Primo, J.; Bach, J. F. CD3 Antibody-Induced Dominant Self Tolerance in Overtly Diabetic Nod Mice. *J. Immunol.* **1997**, *158*, 2947–2954.
4. Belghith, M.; Bluestone, J. A.; Barriot, S.; Megret, J.; Bach, J. F.; Chatenoud, L. Tgf-Beta-Dependent Mechanisms Mediate Restoration of Self-Tolerance Induced by Antibodies to CD3 in Overt Autoimmune Diabetes. *Nat. Med.* **2003**, *9*, 1202–1208.
5. Kohm, A. P.; Williams, J. S.; Bickford, A. L.; McMahon, J. S.; Chatenoud, L.; Bach, J. F.; Bluestone, J. A.; Miller, S. D. Treatment with Nonmitogenic Anti-CD3 Monoclonal Antibody Induces CD4<sup>+</sup> T Cell Unresponsiveness and Functional Reversal of Established Experimental Autoimmune Encephalomyelitis. *J. Immunol.* **2005**, *174*, 4525–4534.
6. Herold, K. C.; Hagopian, W.; Auger, J. A.; Poumian-Ruiz, E.; Taylor, L.; Donaldson, D.; Gitelman, S. E.; Harlan, D. M.; Xu, D.; Zivin, R. A.; et al. Anti-CD3 Monoclonal Antibody in New-Onset Type 1 Diabetes Mellitus. *N. Eng. J. Med.* **2002**, *346*, 1692–1698.
7. Miller, S. D.; Vanderlugt, C. L.; Lenschow, D. J.; Pope, J. G.; Karandikar, N. J.; Dal Canto, M. C.; Bluestone, J. A. Blockade of Cd28/B7-1 Interaction Prevents Epitope Spreading and Clinical Relapses of Murine EAE. *Immunity* **1995**, *3*, 739–745.
8. Kuchroo, V. K.; Das, M. P.; Brown, J. A.; Ranger, A. M.; Zamvil, S. S.; Sobel, R. A.; Weiner, H. L.; Nabavi, N.; Glimcher, L. H. B7-1 and B7-2 Costimulatory Molecules Differentially Activate the Th1/Th2 Developmental Pathways: Application to Autoimmune Disease Therapy. *Cell* **1995**, *80*, 707–718.
9. Karpus, W. J.; Lukacs, N. W.; McRae, B. L.; Streiter, R. M.; Kunkel, S. L.; Miller, S. D. An Important Role for the Chemokine Macrophage Inflammatory Protein-1 Alpha in the Pathogenesis of the T Cell-Mediated Autoimmune Disease, Experimental Autoimmune Encephalomyelitis. *J. Immunol.* **1995**, *155*, 5003–5010.
10. Ruddle, N. H.; Bergman, C. M.; McGrath, K. M.; Lingeheld, E. G.; Grunnet, M. L.; Padula, S. J.; Clark, R. B. An Antibody to Lymphotoxin and Tumor Necrosis Factor Prevents Transfer of Experimental Allergic Encephalomyelitis. *J. Exp. Med.* **1990**, *172*, 1193–1200.
11. Yednock, T. A.; Cannon, C.; Fritz, L. C.; Sanchez-Madrid, F.; Steinman, L.; Karin, N. Prevention of Experimental Autoimmune Encephalomyelitis by Antibodies against  $\beta 1$  Integrin. *Nature* **1992**, *356*, 63–66.
12. Miller, D. H.; Khan, O. A.; Sheremata, W. A.; Blumhardt, L. D.; Rice, G. P.; Libonati, M. A.; Willmer-Hulme, A. J.; Dalton, C. M.; Miszkiel, K. A.; O'Connor, P. W. A Controlled Trial of Natalizumab for Relapsing Multiple Sclerosis. *N. Eng. J. Med.* **2003**, *348*, 15–23.
13. Langer-Gould, A.; Atlas, S. W.; Green, A. J.; Bollen, A. W.; Pelletier, D. Progressive Multifocal Leukoencephalopathy in a Patient Treated with Natalizumab. *N. Eng. J. Med.* **2005**, *353*, 375–381.
14. Klotz, L.; Wiendl, H. Monoclonal Antibodies in Neuroinflammatory Diseases. *Expert Opin. Biol. Ther.* **2013**, *13*, 831–846.
15. Kleinschmidt-DeMasters, B. K.; Tyler, K. L. Progressive Multifocal Leukoencephalopathy Complicating Treatment with Natalizumab and Interferon Beta-1a for Multiple Sclerosis. *N. Eng. J. Med.* **2005**, *353*, 369–374.
16. Kitsos, D. K.; Tsiodras, S.; Stamboulis, E.; Voumvourakis, K. I. Rituximab and Multiple Sclerosis. *Clin. Neuropharmacol.* **2012**, *35*, 90–96.
17. Miller, S. D.; Turley, D. M.; Podojil, J. R. Antigen-Specific Tolerance Strategies for the Prevention and Treatment of Autoimmune Disease. *Nat. Rev. Immunol.* **2007**, *7*, 665–677.
18. Luo, X.; Herold, K. C.; Miller, S. D. Immunotherapy of Type 1 Diabetes: Where Are We and Where Should We Be Going? *Immunity* **2010**, *32*, 488–499.
19. Bielekova, B.; Goodwin, B.; Richert, N.; Cortese, I.; Kondo, T.; Afshar, G.; Gran, B.; Eaton, J.; Antel, J.; Frank, J. A.; et al. Encephalitogenic Potential of the Myelin Basic Protein Peptide (Amino Acids 83–99) in Multiple Sclerosis: Results of a Phase II Clinical Trial with an Altered Peptide Ligand. *Nat. Med.* **2000**, *6*, 1167–1175.
20. Wraith, D. C.; Smilek, D. E.; Mitchell, D. J.; Steinman, L.; McDevitt, H. O. Antigen Recognition in Autoimmune Encephalomyelitis and the Potential for Peptide-Mediated Immunotherapy. *Cell* **1989**, *59*, 247–255.
21. Nicholson, L. B.; Greer, J. M.; Sobel, R. A.; Lees, M. B.; Kuchroo, V. K. An Altered Peptide Ligand Mediates Immune Deviation and Prevents Autoimmune Encephalomyelitis. *Immunity* **1995**, *3*, 397–405.
22. Kennedy, M. K.; Tan, L. J.; Dal Canto, M. C.; Tuohy, V. K.; Lu, Z. J.; Trotter, J. L.; Miller, S. D. Inhibition of Murine Relapsing Experimental Autoimmune Encephalomyelitis by Immune Tolerance to Proteolipid Protein and Its Encephalitogenic Peptides. *J. Immunol.* **1990**, *144*, 909–915.
23. Tan, L. J.; Kennedy, M. K.; Miller, S. D. Regulation of the Effector Stages of Experimental Autoimmune Encephalomyelitis Via Neuroantigen-Specific Tolerance Induction. II. Fine Specificity of Effector T Cell Inhibition. *J. Immunol.* **1992**, *148*, 2748–2755.
24. Getts, D. R.; Turley, D. M.; Smith, C. E.; Harp, C. T.; McCarthy, D.; Feeney, E. M.; Getts, M. T.; Martin, A. J.; Luo, X.; Terry, R. L.; et al. Tolerance Induced by Apoptotic Antigen-Coupled Leukocytes Is Induced by Pd-L1+ and IL-10-Producing Splenic Macrophages and Maintained by T Regulatory Cells. *J. Immunol.* **2011**, *187*, 2405–2417.
25. Vanderlugt, C. L.; Eagar, T. N.; Neville, K. L.; Nikcevich, K. M.; Bluestone, J. A.; Miller, S. D. Pathologic Role and Temporal Appearance of Newly Emerging Autoepitopes in Relapsing Experimental Autoimmune Encephalomyelitis. *J. Immunol.* **2000**, *164*, 670–678.
26. Lutterotti, A.; Yusef, S.; Sputtek, A.; Sturner, K.; Stellmann, J.-P.; Breiden, P.; Reinhardt, S.; Schulze, C.; Bester, M.; Heesen, C.; et al. Antigen-Specific Tolerance by Autologous Myelin Peptide-Coupled Cells: A Phase 1 Trial in Multiple Sclerosis. *Sci. Transl. Med.* **2013**, *5*, 188ra75.
27. Getts, D. R.; Martin, A. J.; McCarthy, D. P.; Terry, R. L.; Hunter, Z. H.; Yap, W. T.; Getts, M. T.; Pleiss, M.; Luo, X.; King, N. J. C.; et al. Microparticles Bearing Encephalitogenic Peptides

- Induce T-Cell Tolerance and Ameliorate Experimental Autoimmune Encephalomyelitis. *Nat. Biotechnol.* **2012**, *30*, 1217–1224.
28. Turley, D. M.; Miller, S. D. Peripheral Tolerance Induction Using Ethylenecarbodiimide-Fixed ApCs Uses Both Direct and Indirect Mechanisms of Antigen Presentation for Prevention of Experimental Autoimmune Encephalomyelitis. *J. Immunol.* **2007**, *178*, 2212–2220.
  29. Viorritto, I. C.; Nikolov, N. P.; Siegel, R. M. Autoimmunity versus Tolerance: Can Dying Cells Tip the Balance? *Clin. Immunol.* **2007**, *122*, 125–134.
  30. Lutsiak, M. E.; Kwon, G. S.; Samuel, J. Biodegradable Nanoparticle Delivery of a Th2-Biased Peptide for Induction of Th1 Immune Responses. *J. Pharm. Pharmacol.* **2006**, *58*, 739–747.
  31. Batanero, E.; Barral, P.; Villalba, M.; Rodriguez, R. Biodegradable Poly (DL-Lactide Glycolide) Microparticles as a Vehicle for Allergen-Specific Vaccines: A Study Performed with Ole E 1, the Main Allergen of Olive Pollen. *J. Immunol. Methods* **2002**, *259*, 87–94.
  32. McCarthy, D. P.; Richards, M. H.; Miller, S. D. Mouse Models of Multiple Sclerosis: Experimental Autoimmune Encephalomyelitis and Theiler's Virus-Induced Demyelinating Disease. *Methods Mol. Biol.* **2012**, *900*, 381–401.
  33. McMahon, E. J.; Bailey, S. L.; Castenada, C. V.; Waldner, H.; Miller, S. D. Epitope Spreading Initiates in the CNS in Two Mouse Models of Multiple Sclerosis. *Nat. Med.* **2005**, *11*, 335–339.
  34. Smith, C. E.; Eagar, T. N.; Strominger, J. L.; Miller, S. D. Differential Induction of IgE-Mediated Anaphylaxis after Soluble vs Cell-Bound Tolerogenic Peptide Therapy of Autoimmune Encephalomyelitis. *Proc. Natl. Acad. Sci. U.S.A.* **2005**, *102*, 9595–9600.
  35. Kutscher, H. L.; Gao, D.; Li, S.; Massa, C. B.; Cervelli, J.; Deshmukh, M.; Joseph, L. B.; Laskin, D. L.; Sinko, P. J. Toxicodynamics of Rigid Polystyrene Microparticles on Pulmonary Gas Exchange in Mice: Implications for Microemboli-Based Drug Delivery Systems. *Toxicol. Appl. Pharmacol.* **2013**, *266*, 214–223.
  36. Getts, D. R.; Terry, R. L.; Getts, M. T.; Deffrasnes, C.; Muller, M.; van Vredent, C.; Ashurst, T. M.; Chami, B.; McCarthy, D. P.; Wu, H.; et al. Therapeutic Inflammatory Monocyte Modulation Using Immune-Modifying Microparticles. *Sci. Transl. Med.* **2014**, *6*, No. 219ra7.
  37. Chong, C. S.; Cao, M.; Wong, W. W.; Fischer, K. P.; Addison, W. R.; Kwon, G. S.; Tyrrell, D. L.; Samuel, J. Enhancement of T Helper Type 1 Immune Responses against Hepatitis B Virus Core Antigen by PLGA Nanoparticle Vaccine Delivery. *J. Controlled Release* **2005**, *102*, 85–99.
  38. Nixon, D. F.; Hioe, C.; Chen, P. D.; Bian, Z.; Kuebler, P.; Li, M. L.; Qiu, H.; Li, X. M.; Singh, M.; Richardson, J.; et al. Synthetic Peptides Entrapped in Microparticles Can Elicit Cytotoxic T Cell Activity. *Vaccine* **1996**, *14*, 1523–1530.
  39. Jenkins, M. K.; Schwartz, R. H. Antigen Presentation by Chemically Modified Splenocytes Induces Antigen-Specific T Cell Unresponsiveness *In Vitro* and *In Vivo*. *J. Exp. Med.* **1987**, *165*, 302–319.
  40. Keegan, M. E.; Falcone, J. L.; Leung, T. C.; Saltzman, M. Biodegradable Microspheres with Enhanced Capacity for Covalently Bound Surface Ligands. *Macromolecules* **2004**, *37*, 9979–9784.
  41. Champion, J. A.; Mitragotri, S. Role of Target Geometry in Phagocytosis. *Proc. Natl. Acad. Sci. U.S.A.* **2006**, *103*, 4930–4934.
  42. Areschoug, T.; Gordon, S. Scavenger Receptors: Role in Innate Immunity and Microbial Pathogenesis. *Cell. Microbiol.* **2009**, *11*, 1160–1169.
  43. Dobrovolskaia, M. A.; McNeil, S. E. Immunological Properties of Engineered Nanomaterials. *Nat. Nanotechnol.* **2007**, *2*, 469–478.
  44. Sahoo, S. K.; Panyam, J.; Prabha, S.; Labhasetwar, V. Residual Polyvinyl Alcohol Associated with Poly(D,L-lactide-co-glycolide) Nanoparticles Affects Their Physical Properties and Cellular Uptake. *J. Controlled Release* **2002**, *82*, 105–114.
  45. Rodriguez, P. L.; Harada, T.; Christian, D. A.; Pantano, D. A.; Tsai, R. K.; Discher, D. E. Minimal "Self" Peptides That Inhibit Phagocytic Clearance and Enhance Delivery of Nanoparticles. *Science* **2013**, *339*, 971–975.
  46. Lundqvist, M.; Stigler, J.; Elia, G.; Lynch, I.; Cedervall, T.; Dawson, K. A. Nanoparticle Size and Surface Properties Determine the Protein Corona with Possible Implications for Biological Impacts. *Proc. Natl. Acad. Sci. U.S.A.* **2008**, *105*, 14265–14270.
  47. Kobayashi, N.; Kobayashi, H.; Gu, L.; Malefyt, T.; Siahaan, T. J. Antigen-Specific Suppression of Experimental Autoimmune Encephalomyelitis by a Novel Bifunctional Peptide Inhibitor. *J. Pharmacol. Exp. Ther.* **2007**, *322*, 879–886.
  48. Zhao, H.; Kiptoo, P.; Williams, T. D.; Siahaan, T. J.; Topp, E. M. Immune Response to Controlled Release of Immunomodulating Peptides in a Murine Experimental Autoimmune Encephalomyelitis (EAE) Model. *J. Controlled Release* **2010**, *141*, 145–152.
  49. Huang, L.; Lemos, H. P.; Li, L.; Li, M.; Chandler, P. R.; Baban, B.; McGaha, T. L.; Ravishankar, B.; Lee, J. R.; Munn, D. H.; et al. Engineering DNA Nanoparticles as Immunomodulatory Reagents That Activate Regulatory T Cells. *J. Immunol.* **2012**, *188*, 4913–4920.
  50. Yeste, A.; Nadeau, M.; Burns, E. J.; Weiner, H. L.; Quintana, F. J. Nanoparticle-Mediated Codelivery of Myelin Antigen and a Tolerogenic Small Molecule Suppresses Experimental Autoimmune Encephalomyelitis. *Proc. Natl. Acad. Sci. U.S.A.* **2012**, *109*, 11270–11275.
  51. Jager, A.; Dardalhon, V.; Sobel, R. A.; Bettelli, E.; Kuchroo, V. K. Th1, Th17, and Th9 Effector Cells Induce Experimental Autoimmune Encephalomyelitis with Different Pathological Phenotypes. *J. Immunol.* **2009**, *183*, 7169–7177.
  52. Tompkins, S. M.; Padilla, J.; Dal Canto, M. C.; Ting, J. P.; Van Kaer, L.; Miller, S. D. De Novo Central Nervous System Processing of Myelin Antigen Is Required for the Initiation of Experimental Autoimmune Encephalomyelitis. *J. Immunol.* **2002**, *168*, 4173–4183.
  53. Bailey, S. L.; Schreiner, B.; McMahon, E. J.; Miller, S. D. CNS Myeloid DCs Presenting Endogenous Myelin Peptides Preferentially Polarize CD4(+) T(H)-17 Cells in Relapsing EAE. *Nat. Immunol.* **2007**, *8*, 172–180.